

Review

Recent Advances in Fiber-Shaped Electronic Devices for Wearable Applications

Minji Kang ¹  and Tae-Wook Kim ^{2,*} 

¹ Chemical Materials Solutions Center, Korea Research Institute of Chemical Technology, 141 Gajeong-ro, Yuseong-gu, Daejeon 34114, Korea; mj kang@kriect.re.kr

² Department of Flexible and Printable Electronics, LANL-CBNU Engineering Institute-Korea, Jeonbuk National University, 567 Baekje-daero, Deokjin-gu, Jeonju 54896, Korea

* Correspondence: twk@jbnu.ac.kr

Abstract: Fiber electronics is a key research area for realizing wearable microelectronic devices. Significant progress has been made in recent years in developing the geometry and composition of electronic fibers. In this review, we present that recent progress in the architecture and electrical properties of electronic fibers, including their fabrication methods. We intensively investigate the structural designs of fiber-shaped devices: coaxial, twisted, three-dimensional layer-by-layer, and woven structures. In addition, we introduce remarkable applications of fiber-shaped devices for energy harvesting/storage, sensing, and light-emitting devices. Electronic fibers offer high potential for use in next-generation electronics, such as electronic textiles and smart integrated textile systems, which require excellent deformability and high operational reliability.

Keywords: electronic fiber; wearable electronics; electronic textiles; fiber electronics



Citation: Kang, M.; Kim, T.-W. Recent Advances in Fiber-Shaped Electronic Devices for Wearable Applications. *Appl. Sci.* **2021**, *11*, 6131. <https://doi.org/10.3390/app11136131>

Academic Editor: Paolo Visconti

Received: 31 May 2021

Accepted: 28 June 2021

Published: 1 July 2021

Publisher's Note: MDPI stays neutral with regard to jurisdictional claims in published maps and institutional affiliations.



Copyright: © 2021 by the authors. Licensee MDPI, Basel, Switzerland. This article is an open access article distributed under the terms and conditions of the Creative Commons Attribution (CC BY) license (<https://creativecommons.org/licenses/by/4.0/>).

1. Introduction

Electronic fiber is a building block of electronic textiles (e-textiles) for developing wearable electronics. In practical applications, fiber-shaped devices have attracted great attention as a potential alternative to conventional planar-type electronic devices. Because of their structural features, which enable them to be sewn into various fabrics, electronic fibers are an ideal device platform for realizing the three-dimensional (3D) deformability, light weight, breathability, washability, and comfort required for e-textiles [1–3]. Their one-dimensional (1D) shape allows fiber devices to maintain their electronic functions under various kinds of mechanical deformation and stimuli. Moreover, electronic devices with different functionalities can be fabricated onto a 1D substrate, and monofunctional fibers can be woven together into an integrated device or e-textile [4]. The use of such fiber technologies will allow various electronic systems for computing, information technology, and communications to be easily incorporated in e-textiles, which can accommodate diverse functional fibers into an unlimited number of structures. For example, smart integrated textiles can be used to process and digitize mechanical, chemical, electrical, and thermal data gathered by fiber units that sense and react to the human body and the environment [5].

Recently, fiber electronics have advanced rapidly with the development of flexible electronics, stimuli-responsive sensors, and soft electronic materials. Unlike conventional electronic devices, electronic fibers require diverse fabrication methods, such as fused printing, spinning, electrodeposition, chemical vapor deposition, casting, rolling, molding, and thermal drawing [1,6–13]. These scalable fabrication processes have themselves been developed to achieve more precise patterning and uniform deposition of the active materials. Improvements in fiber technology have allowed basic device units to be produced in fiber form. The shape, composition, and architecture of electronic fibers can be adjusted

by using suitable soft materials and fabrication processes to optimize function and performance [4,14]. With the rise of smart clothing and artificial intelligence (AI) technology, functional fibers with sensing, computing, memory, energy storage, energy-harvesting, and display capabilities have attracted much interest in the fiber industry [5]. In response to the demand for deformable devices, various types of fiber-shaped electronic components have been successfully developed, including transistors, memory devices, memristors, artificial synapses, sensors, light-emitting diodes (LEDs), and energy devices. To investigate the practical applications of these fiber-shaped devices, researchers have woven them into fabrics and integrated them into textiles [5].

In this review, we summarize recent research in electronic fibers with fiber-shaped energy storage and harvesting devices, and smart integrated electronic textile systems. We introduce the structures and structural features of electronic fibers in Section 2. The potential applications of and feasible approaches to fiber-shaped devices, including newly developed fabrication techniques and production processes, are explained in Section 3 to highlight the research and development still required to realize smart fiber systems. In Section 4, we discuss recent advances in multi-functional fibers and e-textiles. Finally, we consider the challenges and issues that need to be solved in the development of fiber-shaped electronic devices and smart textile systems.

2. Device Structure of Electronic Fibers

Compared with conventional planar devices on a two-dimensional (2D) substrate, fiber-shaped devices exhibit good breathability, wet permeability, and hygroscopicity, making them comfortable to wear. The one-dimensional (1D) form of a fiber-shaped device offers excellent flexibility and a light weight, and can accommodate large strain deformations, such as the stretching, 3D bending, and 3D twisting caused by human motion [15]. Moreover, fiber-shaped devices can easily be integrated with other functional fibers using conventional weaving processes.

Fiber-shaped devices have mainly been fabricated into four representative structures: coaxial, twisted, three-dimensional layer-by-layer (3D LBL), and woven (Figure 1) [16]. The coaxial structure is a three-dimensional linear structure, like an electrical cable, composed of an inner electrode core surrounded by active materials and outer electrodes (sometimes with an encapsulation layer) (Figure 1a). Solution-based printing is the main fabrication method for coaxial fiber devices, and it can be scaled up to reel-to-reel manufacturing. However, uniformly placing thin films onto flexible and deformable fiber substrates remains challenging. It is also difficult to stack active materials in layers, and to create patterned layers or fully covered films without causing defects to the single fibers.

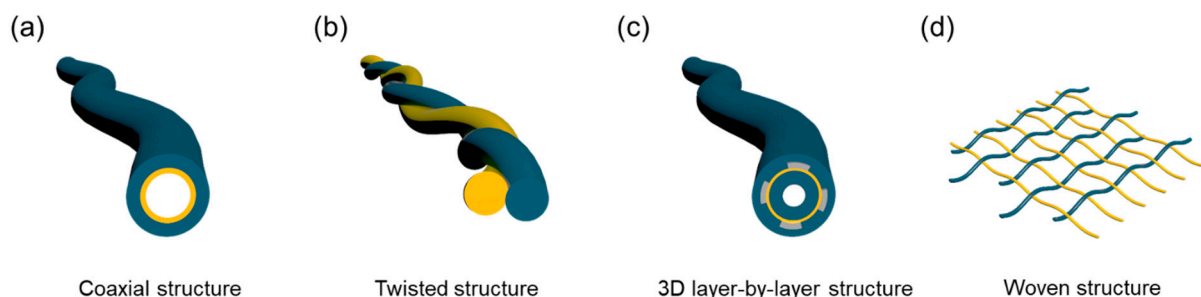


Figure 1. Schematics of representative device structures of (a–c) 1D electronic fibers and (d) 2D electronic textiles.

Another design strategy for single-fiber devices is a twisted structure (Figure 1b). Two or more single fibers containing different components are twisted together to fabricate a 1D device in one direction. In general, the twisting process uses both a rotating stage and a rotor. For instance, one end of a functional fiber can be attached to a feeding roller positioned at a specific angle, and the other can be attached to a fiber electrode that is fixed to a motor. The motor in the twister machine begins to move, and the single fibers are plied

together. The twisted structure minimizes fiber divergence and increases the interface area between the electrode and the functional fibers. However, the tightness affects the twisting stress; thus, the contact force decreases as the degree of twist decreases. Furthermore, repetitive folding and bending could loosen the twist structure.

A 3D LBL structure is similar to a 3D sandwich configuration, in which two or more electrodes are separated by an active layer (Figure 1c). All components are integrated into a single fiber; thus, the 3D LBL structure enables particularly small device dimensions. The fixed electrode layers prevent physical disconnection between the active layer and the electrode. In this way, the 3D LBL single-fiber structure provides better structural stability against external physical deformation than the twisted and interlaced fiber structures [17]. 3D LBL devices can be customized to the needs of particular applications via thermal drawing methods [13]. The geometry and architecture of 3D LBL devices are tunable within a single fiber; moreover, discrete device units can be embedded into the preform. In this regard, monolithic integration of multiple functionalities in a 3D LBL electronic fiber can be demonstrated by increasing the density of devices [18].

Most e-textiles are made by interdigitating and interpenetrating different types of 1D electronic fibers. A representative device structure of 2D e-textiles is shown in Figure 1d. Electronic fibers can be designed to hold diverse patterns in 2D textile structures. Two fiber devices can share fiber electrodes in a textile and integrate different functions. For example, fiber-shaped supercapacitors (or batteries) can be integrated with fibriform solar cells (or nanogenerators) in one fabric for simultaneous energy storage and harvesting [17]. Although the integration of electronic fibers has mainly been achieved through weaving, threading, knitting, or by hand, some fiber devices are easily damaged by traditional textile processes. Therefore, automatic processing technologies that can produce well-aligned arrays and robust interconnections between electronic fibers and electrodes have been developed to construct scalable e-textiles [19,20].

3. Device Applications

In this section, we focus on recent research about directly integrating fibriform electronic devices into textiles, apart from attaching electronic components. Monolithic integration could potentially simplify the manufacturing process and improve user comfort. Integrating analog and digital microelectronics into textiles has attracted significant attention, but the integrating of electronic functions into a textile structure while retaining the mechanical properties of the textile still requires a great deal of effort.

3.1. Electronic Devices

3.1.1. Transistors

Transistors are one of the key electrical components of integrated electronic circuits that amplify and convert electrical signals simultaneously. They can also be applied to a variety of optoelectronic devices, such as displays, integrated circuits (ICs), memory devices, synaptic devices, and sensors. To date, most transistors have been fabricated on planar and rigid substrates. The development of flexible fiber-shaped transistors to give fabrics computational ability is still at an early stage because of the ongoing challenges involved in forming uniform films and high-resolution patterning on fiber substrates, and interconnecting fiber electrodes [2]. Thus, fabrication methods for electronic fibers and textile-compatible technology have been chosen as the primary focus of this research area.

Fiber-shaped transistors have mainly been fabricated using mechanically flexible materials with a coaxial structure. The dielectric, semiconductor, and electrode materials are sequentially coated onto an electrode core using solution (dip-coating, spray, etc.) and vapor processes (sputtering, atomic layer deposition, chemical vapor deposition, etc.) [21,22]. Various semiconducting materials have been applied to create a fibriform channel layer, such as polymers [23,24], organic small molecules [3,21,25], single-walled carbon nanotubes (SWCNTs) [23,26], and metal oxides [27,28]. For instance, Kim et al. fabricated organic field-effect transistor (OFET) fibers on Au microwires (Figure 2a) [29]. The OFET fiber was made from

a coaxial bi-layer composed of 2,8-difluoro-5,11-bis (triethylsilylethynyl)anthradithiophene (diF-TESADT) as an organic semiconductor and poly(methyl methacrylate) (PMMA) as the insulating polymer [29]. The diF-TESADT: PMMA blend solution was coaxially die-coated and solidified with vertical phase-separation. The dimension of the spirally wrapped CNT microelectrodes was controlled using a rolling-transfer method, and the OFET fiber showed a maximum field-effect mobility of $0.68 \text{ cm}^2\text{V}^{-1}\text{s}^{-1}$ and good output current characteristics [29]. 2D crystals of organic small molecules (2DCOS) were used to fabricate fibriform OFETs through a jigsaw-puzzle physical-chemical method [25]. 2DCOS film was prepared using a solution epitaxy method, and then transferred onto a planar substrate to fabricate the OFETs [25]. The 2DCOS-based FETs were then peeled off and attached to the target fibers. The 2DCOS fiber transistors showed competitive electronic characteristics: a high field-effect mobility of $1 \text{ cm}^2\text{V}^{-1}\text{s}^{-1}$, well-balanced ambipolarity via the p–n junction, high inverter gain up to 12.4, and a near-infrared photoresponsivity of $1.06 \times 10^4 \text{ A W}^{-1}$, with photodetectivity of 10^{13} Jones [25]. Heo et al. reported reel-processed 1D complementary metal-oxide-semiconductor (CMOS) logic circuits based on SWCNT transistors (Figure 2b) [22]. P- and n-type SWCNT fiber transistors were demonstrated using selectively chemical doping and a photochemical patterning technique [22]. The device exhibited high hole mobility of $4.03 \text{ cm}^2\text{V}^{-1}\text{s}^{-1}$ (electron mobility of $2.15 \text{ cm}^2\text{V}^{-1}\text{s}^{-1}$) and a gain of 6.76 with good dynamic operation at an applied voltage of 5.0 V [22]. Park et al. also fabricated fiber-shaped FETs with an $\text{Al}_2\text{O}_3\text{–MgO}$ nanolaminate insulator and an In–Ga–Zn–O (IGZO) semiconductor [27]. The $\text{Al}_2\text{O}_3\text{–MgO}$ and IGZO layers were deposited using a thermal atomic layer deposition system and radio-frequency sputtering, respectively [27]. The resulting fiber-shaped IGZO FETs exhibited an on- and off-current ratio above 10^8 and good electron mobility of more than $3 \text{ cm}^2\text{V}^{-1}\text{s}^{-1}$ with a leakage off-current of less than 10^{-9} A [27].

Many obstacles continue to limit the practicality of using 1D FETs for electronic circuits. One of the main issues is that 1D FETs still require sophisticated fabrication techniques that demand a vacuum process such as thermal evaporation, sputtering, or atomic layer deposition, which is unsuitable for commercialization [30]. Moreover, the high operating voltages required by OFETs, along with their low conductance values and unstable electrode interconnections, need to be resolved. In this regard, a new device design strategy has been developed for high-performance 1D FETs. Kim et al. fabricated fibrous OFETs with a twisted structure and a solid ion-gel electrolyte (Figure 2c) [30]. The source and drain (S/D) fiber electrodes were coated with an organic semiconductor and twisted together. The twisted assembly of electrode fibers was then surrounded by an ion gel, and the gate wire was then wound around that [30]. The resulting fibrous OFETs achieved milliamperes-level output current and a good on/off ratio of 10^5 at low gate voltages (below -1.3 V) [30]. Their work reveals a promising structural strategy that could help overcome the current limitations of coaxial fiber FETs.

As another class of fiber transistors for wearable electronic devices, fiber-shaped organic electrochemical transistors (OECTs) have been explored because they can simplify the complex manufacturing processes required for coaxial fiber OFETs [24,31]. The OECTs use an electrolyte instead of an insulating layer of FETs, and therefore they do not need a smooth fiber substrate [31]. By applying a gate voltage, ions are injected from the electrolyte into the top surface or inner part of the semiconducting film, thereby doping the channel [32]. However, OECTs operated by doping/de-doping conducting polymers can work only in the depletion mode, and the response time is longer than that of OFETs due to slow ion transport in the ionic liquid [32]. Hamedi et al. demonstrated electric double-layer capacitor-gated (EDLC) transistors on sputter-coated metal fibers using poly(3-hexylthiophene) (P3HT) and imidazolium ionic liquid [11]. In the EDLC-OFETs, the channel conductivity was modulated by electrolyte polarization upon exposure to an electric field [11]. Therefore, the demonstrated EDLC transistors operated below 1 V and exhibited large current densities and improved switching speeds [11]. Owyung et al. also demonstrated CNT transistors on linen threads, using a colloidal silica-based ionic

liquid gel that induced all-around electrostatic gating (Figure 2d) [26]. The thread substrate was knotted with S/D Au wire, and then the P3HT (or CNT) semiconductors and ionogel were sequentially deposited by drop casting onto the thread [26]. These ionogel-gated transistors were applied as a switch and a multiplexed diagnostic device with simple logic gates (NAND, NOR, and NOT) [26].

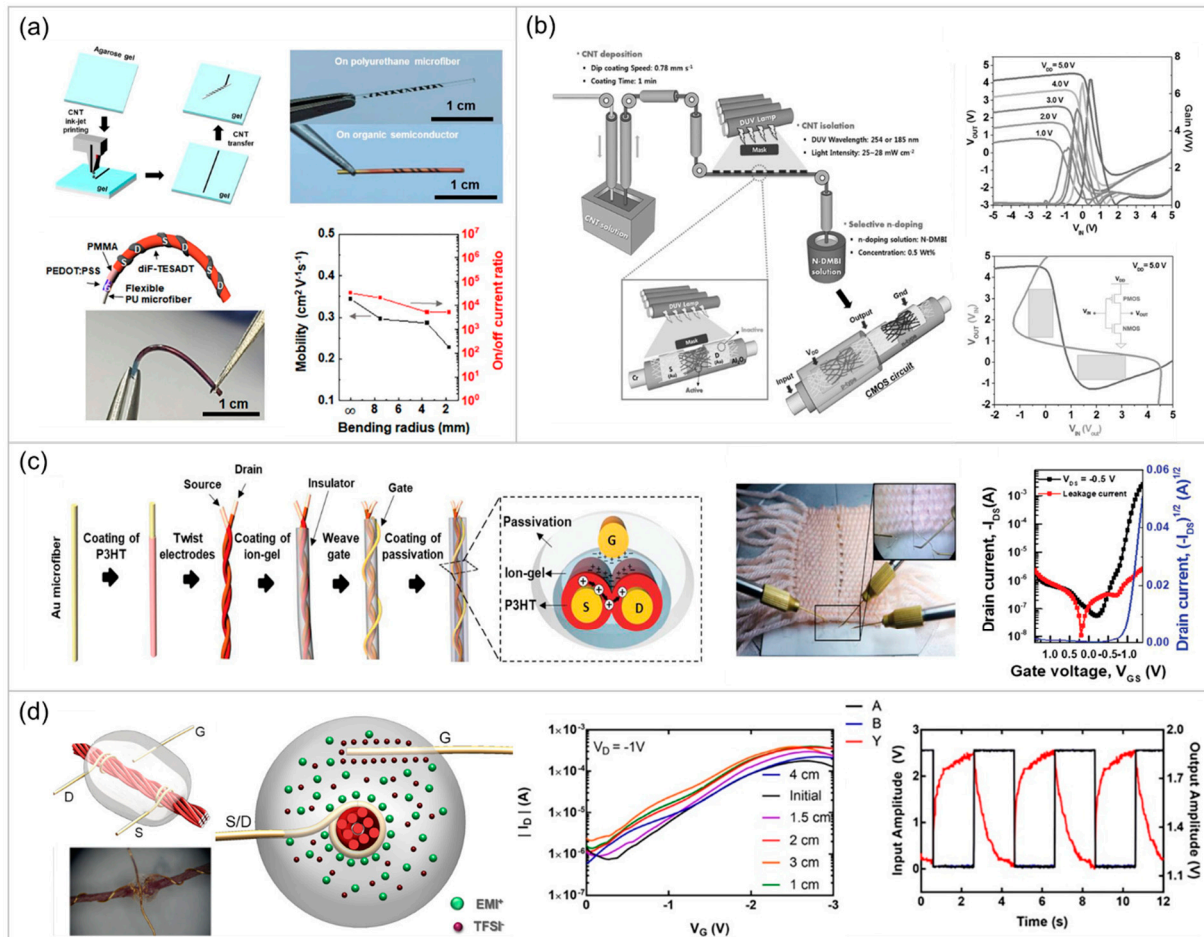


Figure 2. (a) Top: schematic of the rolling-transfer process of printed CNT microelectrodes (left) and photographs of the spirally wrapped CNT microelectrodes on fiber substrates (right). Bottom: schematic and photograph of a flexible fiber OFET (left), field-effect mobilities and on/off current ratio with various bending radii (right). Reproduced with permission Ref. [29]. Copyright 2020, American Chemical Society. (b) Left: schematic illustration of a fabrication process for fiber-shaped CMOS circuitry. Right: electrical properties of the 1D complementary inverters. Reproduced with permission Ref. [22]. Copyright 2017, Wiley-VCH. (c) Left: schematic illustration of a fabrication process of a fiber-shaped OFET with the twisted structure and a solid ion-gel electrolyte. Right: photograph and transfer characteristics of the fiber-shaped OFET embedded in a fabric. Reproduced with permission Ref. [30]. Copyright 2019, Wiley-VCH. (d) Left: schematic illustration and photograph of the ionogel-gated fiber transistor. Middle: transfer characteristics of the ionogel-gated transistor with different bending radii. Right: electrical characteristics of logic gate NAND (A and B curves: two logic gate inputs, Y curve: output from the circuit). Reproduced with permission Ref. [26]. Copyright 2019, American Chemical Society.

Electrochemical and electrolyte-gated transistors can easily be integrated into woven circuitry in textiles and operated at low voltages. However, the low reliability in switching behavior under chemical and bias stress must be improved before their application will be practical. For this reason, highly reliable electrolyte-based materials should be developed.

3.1.2. Memory Devices

Electronic memory is an essential element of electronic circuits that store information. To store electronic signals generated by wearable processors, sensors, and elec-

tronic circuitry, researchers have fabricated soft and flexible fiber-shaped memory devices. There are two main types of fiber-shaped memory: resistor-type and transistor-type. Kang et al. reported a stretchable resistive memory device using a graphene-poly(3,4-ethylenedioxythiophene):poly(styrene sulfonic acid) (PEDOT:PSS) hybrid material dip-coated on a nylon thread [33]. Conductive filaments were generated by applying voltages to access charges trapped in the graphene flakes [33]. The resulting fiber-shaped memory device has write-once-read-many-times characteristics and a retention time of 10^6 s, with an on/off ratio of approximately 10^3 [33]. Jo and coworkers developed a textile-based resistive switching random access memory (RRAM) [34]. The woven RRAM was fabricated using a carbon counter-electrode fiber and an Al_2O_3 resistance switching layer formed on an Al-coated cotton fiber (Figure 3a) [34]. When the 3×3 RRAM array was embroidered into a cloth, it exhibited stable resistance switching for more than 100 cycles with an on/off ratio exceeding 10^2 (Figure 3b) [34]. In another example, Bae and his colleagues demonstrated a textile memristor array in a logic-in-memory circuit that acted as both nonvolatile memory and a logic gate [35]. Cotton yarn was dip-coated with aluminum as a metallic electrode, and then poly(ethylene glycol) dimethacrylate (pEGDMA) was deposited as a resistive switching layer using an initiated chemical vapor deposition (iCVD) process (Figure 3c) [35]. Two aluminum/pEGDMA layers on the yarn intersected with each other, forming a memristor unit [35]. The pEGDMA memristors were woven in a crossbar array of textile structure, with untreated yarns that acted as cell-to-cell barriers [35]. The fabricated devices showed outstanding nonvolatile memory characteristics, including low operation voltage (<1.5 V), long-term retention ($>1.5 \times 10^7$ s), and good cycling endurance (>500 cycles), mechanical robustness, and washability [35]. The textile memristor crossbar array composed as a logic-in-memory circuit successfully implemented basic Boolean functions, such as half-adder and NOT, NOR, OR, AND, and NAND logic gates (Figure 3d) [35]. The pEGDMA memristor-based crossbar array architecture is one possible application for smart textile systems that use energy-efficient, normally-off computing, which is compatible with the limited battery capacity of wearable devices [35]. These resistor-type memory devices have high integration density and a simple crossbar geometry structure, which is an advantage for production, but they can suffer from undesired cross-talk in ICs [35]. Although that problem can be solved by incorporating supplementary switching elements, this type of complex structure requires additional processes.

Compared with resistor-type fiber memory devices, fibriform transistor-type memory has reliable switching, compatibility with ICs consisting of MOS FETs, and a non-destructive read-out without cross-talk interference between memory units [36]. Kang et al. demonstrated fiber-shaped organic transistor memory devices (FOMs) based on a ferroelectric copolymer of vinylidene fluoride and trifluoroethylene [P(VDF-TrFE)] [3]. The FOMs were fabricated onto a silver (Ag) microwire using a capillary tube-assisted coating method (Figure 3e) [3]. The simple solution process formed smooth and compact nanograined P(VDF-TrFE) films on thin fiber substrates [3]. The resulting FOMs exhibited excellent memory performance with high flexibility, reliable endurance for 100 cycles, and a long-term retention time of $\sim 5 \times 10^4$ s at voltages below 5 V (Figure 3f) [3]. The FOMs, sewn into a stretchable fabric, operated stably when the fabric was subjected to uniaxial and diagonal strain and crumpling [3].

Fiber-shaped transistors and memory devices are far from practical implementation. The contacts in the warps and wefts of electronic fibers in a textile structure are loosened by mechanical stress, which can easily cause the electronic fibers to lose their function. Therefore, it is important to form robust electrical connections between the memory units, and to maintain performance as the electronic fibers are detached and reattached. For further improvement, integration with other functional fibers and new device architectures will be required.

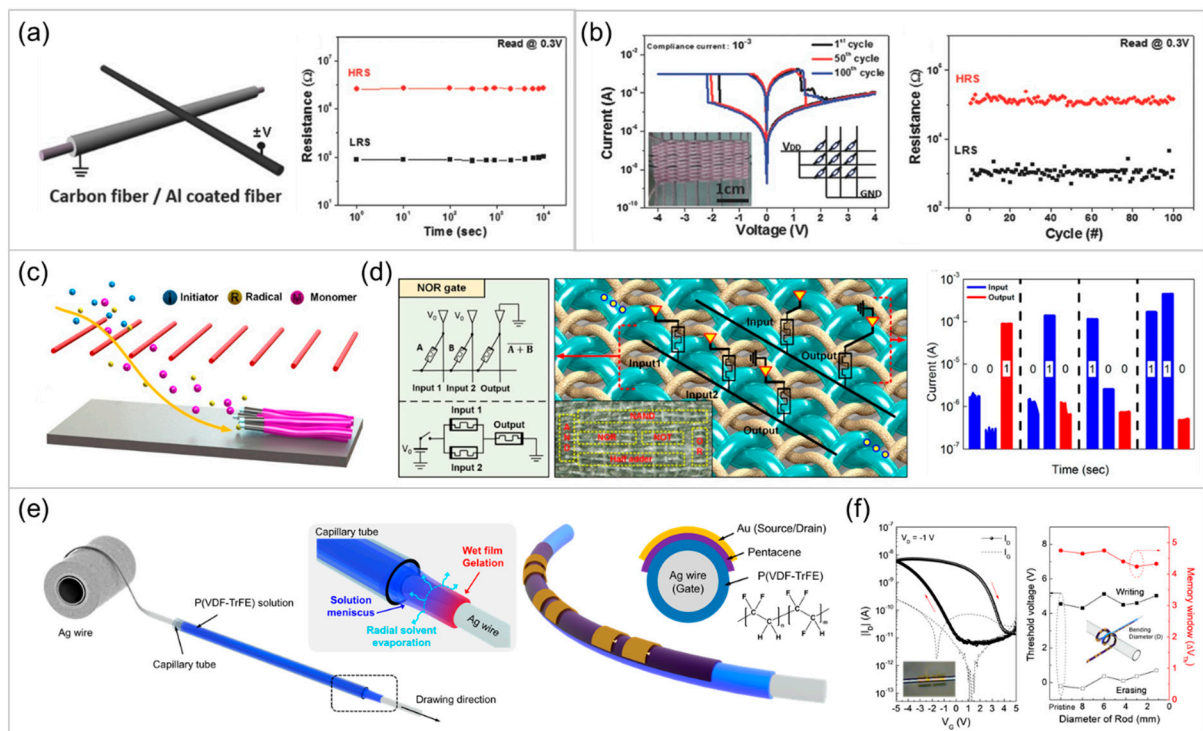


Figure 3. (a) Schematic of the device structure and the retention property of a fiber-shaped memory device (b) Endurance test of a 3×3 RRAM array embroidered into a fabric. (a,b) Reproduced with permission Ref. [34]. Copyright 2017, Wiley-VCH. (c) Schematic illustration of the deposition of pEGDMA using an iCVD process. (d) Left: schematic of the logic-in-memory operations of NOR gate and its equivalent circuits within the crossbar array. The inset presents a conceptual image for the integration of logic gates on the fabric. Right: measurements of the NOR gate. (c,d) Reproduced with permission Ref. [35]. Copyright 2017, American Chemical Society. (e) Schematic illustration of a continuous reel-to-reel coating process and the device structure of the FOMs. (f) Memory and bending characteristics of the FOMs. (e,f) Reproduced with permission Ref. [3]. Copyright 2019, American Chemical Society.

3.1.3. Computing Units

Machine learning for wearable applications is becoming a popular way to study the huge quantities of data accrued during the last few years [37]. Despite advances in fiber devices based on AI, such devices typically depend on cloud servers and physically separated computing systems. In other words, the mass of data generated from electronic fibers or e-textiles should be transferred to another computing component. That process consumes a large amount of energy and time. Therefore, a smart e-textile system that can implement data processing or machine learning is highly desirable [38,39]. One potential method would be to integrate computing fibers within the 1D functional devices [40]. For example, Xu et al. reported interwoven textile memristors compatible with a two-terminal crossbar configuration (Figure 4a) [41]. Deoxyribonucleic acid (DNA) molecules incorporating Ag nanoparticles as a bio-compatible and ionic conducting layer were assembled on metal fibers via electrophoretic deposition [41]. Interlaced with Pt fiber electrodes, the DNA active layer functioned as a textile memristor and had excellent memristive characteristics: low operating voltage (about 0.3 V), fast switching time (20 ns), and low power consumption (about 100 pW) [41]. The edge-on orientation of DNA molecules provided efficient transport pathways for Ag^+ ions, enabling robust performance [41]. These memristive textiles implemented fundamental logic calculations such as implication and NAND, and were integrated with a textile power source and light-emitting modules to demonstrate the feasibility of a wearable information processing system (Figure 4b) [41].

To bypass the von Neumann bottleneck and avoid high power consumption, bio-inspired computing systems have been developed and are considered to be a promising alternative to traditional hardware. Research on artificial synapses, inspired by the function

and structure of the human brain, is constantly being conducted to achieve the required neural computations [42]. So far, two-terminal and three-terminal fiber-shaped artificial synapses have been demonstrated. Park et al. fabricated two-terminal memristor-type artificial synapses comprising two yarns coated with reduced graphene oxide (rGO) by electrochemical deposition [43]. The rGO-based artificial synapses emulated several synaptic functions, such as paired-pulse facilitation, excitatory postsynaptic current, and a transition from short-term plasticity to long-term plasticity [43]. The yarn-based synapses were assembled in a cross-point structure for e-textile application [43]. However, in an integrated synaptic array, the two-terminal structure can induce undesirable neural signals across neighboring nodes, leading to the degradation of learning accuracy [44].

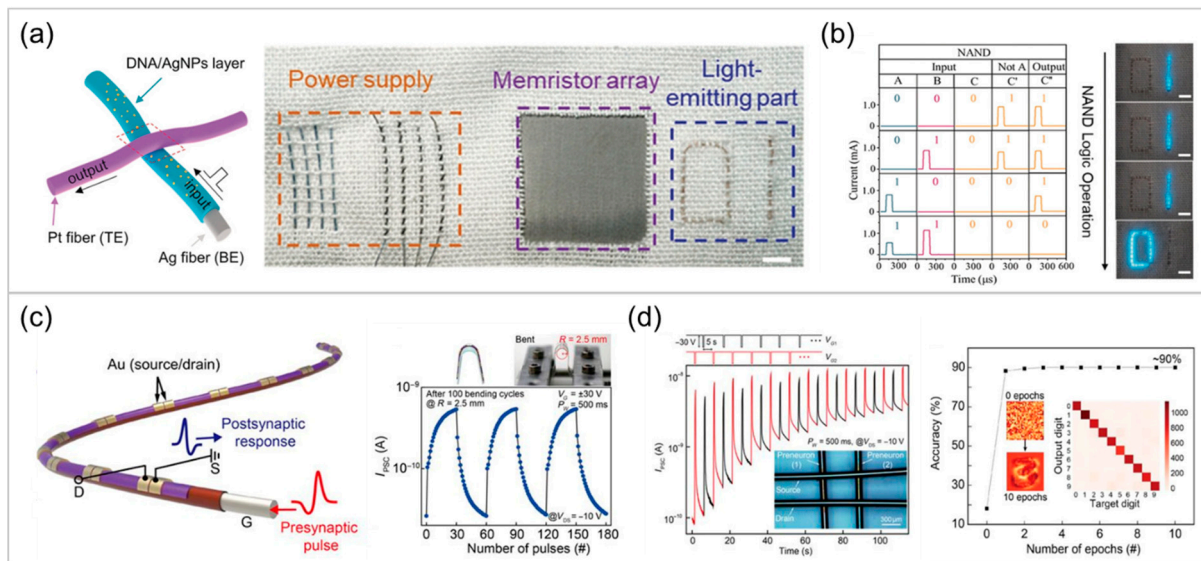


Figure 4. (a) Schematic illustration of a DNA-bridged memristor and photograph of the integration of textile power supply, chip, and light-emitting modules for the textile chip. (b) Left: the basic logic-in-memory function of NAND. Right: photograph of a NAND logic operation in an all-fabric data-processing system. (a,b) Reproduced with permission Ref. [41]. Copyright 2020, Wiley-VCH. (c) Left: schematic illustration of fiber-shaped organic artificial synapses. Right: repetitive transitions of the LTP/LTD of postsynaptic response current (I_{PSC}) at a fixed bending radius ($R = 2.5$ mm). (d) Left: plot of the integrated I_{PSC} in the 2×2 array, with alternately applied current potentiating the two different voltage pulses, with $\Delta t = 5$ s at each preneuron. The inset is a photograph of the 2×2 array. Right: recognition accuracy for MNIST patterns with respect to the number of learning epochs. The left inset presents a reshaped 28×28 contour image of the digit 3 from w before and after 10 epochs, and the right inset shows the confusion matrix for a classification test involving 10,000 MNIST images after 10 epochs. (c,d) Reproduced with permission Ref. [45]. Copyright 2020, American Association for the Advancement of Science (AAAS).

To prevent such cell-to-cell crosstalk and improve the reliability of the learning capability, 1D organic synaptic transistors based on a three-terminal device structure were constructed by Ham et al. (Figure 4c) [45]. Their fiber-shaped multi-synaptic device platform could independently address and transmit neural signals without undesired interference between individual synapses in an e-textile neural network [45]. The 1D artificial synapses were fabricated using P(VDF-TrFE) film dip-coated on a thin Ag wire [45]. They showed essential synaptic functions by modulating the degree of polarization through the electrical stimulus, and their device operated well under bent and coiled states, indicating excellent mechanical stability (Figure 4c) [45]. A NOR-type synaptic array was demonstrated by cross-connecting 1D multi-synapses and Ag fiber electrodes, and the output signals from the individual synapses could be integrated and propagated without significant leakage (Figure 4d) [45]. In particular, recognition accuracies of up to ~ 90 and $\sim 70\%$ were achieved for modified National Institute of Standards and Technology (MNIST) and electrocardiogram (ECG) patterns, respectively (Figure 4d) [45]. The initial accuracy

for the ECG pattern was almost maintained, even under 100 bending cycles at a fixed bending radius of 2.5 mm (error margin: ~2%) [45]. The 1D multi-synapses built as a proof of concept provide a promising approach to the realization of an e-textile neural network for use in a wearable neuromorphic electronic system [45].

Clearly, developments and breakthroughs have been made in the structural designs and capabilities of fiber-shaped computing components. Although a neural textile network that can receive multi-terminal signals and build a high-density artificial neural system has been demonstrated, the processing efficiency should be increased, and fundamental synaptic functions should be accurately mimicked [42].

3.2. Sensing Devices

Wearable 1D sensors have been developed to accurately monitor the environment and health, which can be characterized using various optical, mechanical, and chemical signals [1]. The flexible and compact sensor devices can conform to dynamic and irregularly shaped surfaces to collect high-quality data. This section briefly describes the most widely realized fiber-shaped sensor systems.

Detecting human motion is necessary for medical care, sports science, and rehabilitation [46]. Wearable motion sensors can contribute to the quick diagnosis of characteristic movement disorders, including sudden paralysis and tremors in the body, and to quality care of physical diseases, such as Alzheimer's disease, Parkinson's disease, and diabetes [46]. To track human motion in real time, wearable mechanical sensors that can detect continuous deformation have been developed.

Meng et al. reported a sensing textile system for biomonitoring and interacting over the Internet (Figure 5a,b) [47]. A 3-ply-twisted polyester–silver fiber was made by entwining polyester fibers around a silver wire to form a triboelectric layer and an electrode on a silver-coated polyester fabric (Figure 5c) [47]. The hybrid fibers were stitched onto the silver-coated fabric, where they detected a continuous pulse wave induced by a combination of triboelectrification and electrostatic induction that originated from the fiber when it was mechanically deformed by human skin (Figure 5c) [47]. The textile-based sensor exhibited a high sensitivity of 3.88 V kPa^{-1} in sensing tiny ambient pressure signals, and continuous operation across 80,000 cycles [47]. Based on the sensors, a wireless biomonitoring system (WBS) was developed to collect patients' health data, wirelessly transmit those data, and display the data through an APP interface on a mobile phone (Figure 5d) [47]. The WBS was able to diagnose obstructive sleep apnea and hypopnea syndromes, even with body movements [47]. The textile-based WBS highlights the great potential of smart textiles for personalized health care [47]. The triboelectric fiber device could have applications in a fiber rescue sensor [47]. A 3D honeycomb-structured triboelectric nanogenerator (TENG) based on a flame-retardant wrapping yarn was developed by Li and coworkers [48]. The sustainable and durable single-electrode triboelectric yarn was fabricated through a continuous, hollow-spinning, fancy twister process [48]. The conductive core yarn was wrapped with polyimide yarn for a core–sheath structure [48]. The TENG fibers offer flame retardancy and reduce vibration and noise [48]. Because the fibers can perform both energy harvesting and emergency signal transmission, the woven TENG fabric could be applied to locate a survivor's position in a fire and thereby enable the timely search and rescue of victims [48].

Flexible actuators can convert external energy (heat, light, electricity, humidity, etc.) into mechanical deformation. Wu et al. reported a soft electroactive textile actuator [49]. A fabric electrolyte was coated with PEDOT:PSS conductive ink, doped with SWCNTs, and wired into a zeolite imidazolate framework-8 [49]. The intermediate electrolyte fabric was prepared by immersion in poly (vinylidene fluoride-co-hexafluoropropylene) to increase the ionic conductivity (6.7 mS cm^{-1}) [49]. The resulting textile actuator operated under 3 V at frequencies from 0.1 to 10 Hz and showed a large strain difference of $0.28\% \text{ s}^{-1}$ at 10 Hz and a good blocking force of 0.62 mN at 0.1 Hz, thanks to the high ionic conductivity, large

specific surface area, and good mechanical features of the conducting electrodes based on metal-organic framework derivatives [49].

Ding et al. applied SWCNT/PVA thermoelectric (TE) materials to wearable electronics [50]. The TE materials can convert temperature into an electrical voltage for use as touch sensors, health monitoring, and heat energy harvesting [50]. TE fibers were fabricated using a colloidal gelation extrusion, which is a simple, controllable, industrial, and scalable manufacturing process [50]. When alternating p/n-type TE fibers were woven into fabrics, the TE textiles demonstrated conformal heat energy generation and a multi-pixel touch display panel for hand-writing and communication [50].

Olfaction-like chemical sensors, in which chemical stimuli in a wearable device or the skin are converted into electrical signals, can collect information from their surroundings [51]. The porous and cylindrical structures of fiber-shaped sensors have high active areas, which play a key role in chemical sensing [52]. However, realistically imitating and understanding human-environment interactions remains challenging, due to the limited chemical sensing capabilities of existing sensor technology. As a general interface between humans and their surroundings, textiles could be used to build a sensing platform. To do this, thread-like chemical sensors fabricated using soft, chemically sensitive materials are required.

Real-time health monitoring and the long-term detection of physiological signals are important in disease diagnosis [53,54]. Therefore, fibrous humidity, pH, gas and ion sensors have been developed [55–60]. Notably, Jia et al. fabricated a bioinspired conductive silk microfiber for diagnosis and wound healing in diabetes [61]. The PEDOT silk microfibers were formed using a bioinspired extraction–protection process, and polydopamine was used as an adhesion layer (Figure 5e) [61]. The conductive silk fibers were woven and fabricated into a fibroin patch to monitor physiological signals (Figure 5f) [61]. Thanks to its antioxidant activity, the patch showed good performance in healing chronic diabetic wounds by reducing inflammation and regulating oxidative stress [61].

Ultraviolet (UV) monitoring sensors based on fiber substrates have been demonstrated to detect UV radiation that causes serious skin diseases. A self-powered UV photodetector was developed by Xu et al. [62]. A photoactive CuZnS/TiO₂ nanotube array was formed on a Ti microwire by a two-step anodic oxidation process and a dipping method [62]. A CNT electrode fiber was entwined around the CuZnS/TiO₂ composite nanotube [62]. The fibrous UV sensor exhibited optical responsivity of 2.54 mA W⁻¹ at 0 V, a responsivity of 640 A W⁻¹, and external quantum efficiency of 2.3 × 10⁵ % under 300 nm-UV light irradiation [62]. Furthermore, a real-time wearable UV-sensing fiber that read out UV-light power density and transmitted data to smartphones using wifi was demonstrated [62].

Although fiber-shaped sensors have been studied during the past few years, sensing textiles are still at an early stage of development. For wearable sensing applications, a broad sensitivity range, fast response/recovery, and high sensitivity to diverse physical, chemical, and physiological stimuli are desirable, and reliability must also be improved [37,63].

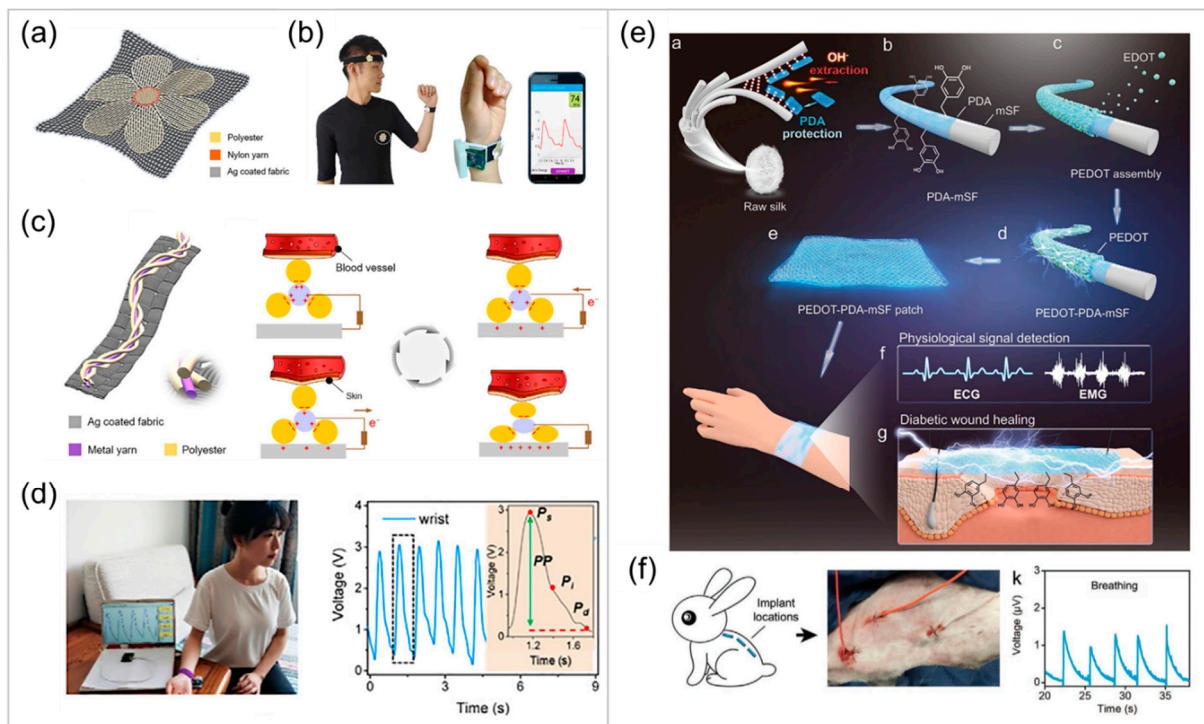


Figure 5. (a) Schematic illustration of the as-fabricated textile-based sensor. (b) Photographs of a wireless biomonitoring system based on a wearable textile sensor. (c) Schematic illustration of a 3D honeycomb-structured triboelectric nanogenerating fiber and working mechanism. (d) The textile-based wireless biomonitoring system and the acquired pulse wave signals when worn by a woman. (a–d) Reproduced with permission Ref. [47]. Copyright 2020, Elsevier. (e) Schematics of the fabrication process and a silk-based patch for diabetic wound healing. (f) A photograph of patches implanted as electrodes in a rabbit's back (left image) and signals detected after breathing. (e,f) Reproduced with permission Ref. [61]. Copyright 2021, Wiley-VCH.

3.3. Light-Emitting Fibers

Fiber-shaped light-emitting devices have attracted great attention. Incorporating fiber LEDs into clothes is expected to maximize human–machine communication [15]. Therefore, fiber LED devices have been developed using inorganic LEDs, organic LEDs (OLEDs), light-emitting electrochemical cells (LECs), and phosphorescent electroluminescent devices (PELDs) [64].

Mi et al. reported ultra-stretchable electroluminescent fibers (up to 400% stretch) that can display a pixel-based controllable light-emitting pattern (Figure 6a) [65]. A dip-coated zinc sulfide (ZnS) electroluminescent layer and a dielectric layer were sandwiched between two liquid metal-coated electrodes (eutectic gallium-indium, EGaIn) [65]. The cross-point of the ZnS-based fiber and the EGaIn-based fiber acted as an electroluminescent pixel that formed an electroluminescent fabric matrix when woven (Figure 6b) [65]. The pixel pattern on the fabric could be displayed using a direct-current (DC)–alternating-current converter connected to a Bluetooth switch in the electric circuit (Figure 6c) [65]. Zhang et al. developed continuous electroluminescent fibers using a one-step extrusion method (Figure 6d) [66]. The outer electroluminescent layer, containing ZnS particles with a silicone elastomer as a protecting layer, was simultaneously extruded with two inner parallel hydrogel electrodes [66]. Because of its unique single-fiber structure, the electroluminescent fibers emitted light in all directions [66]. The luminance of the light-emitting fiber was recoverable at 300% stretch, and retained after 100 stretching cycles [66]. These electroluminescent fibers were woven into a stretchable fabric to produce display patterns (Figure 6e) and applied to implement a brain-interfaced camouflage system (Figure 6f) [66]. The electroluminescent textile reacted to neuronal responses to decoder

lights [66]. The resulting textile display represents a promising wearable communication platform.

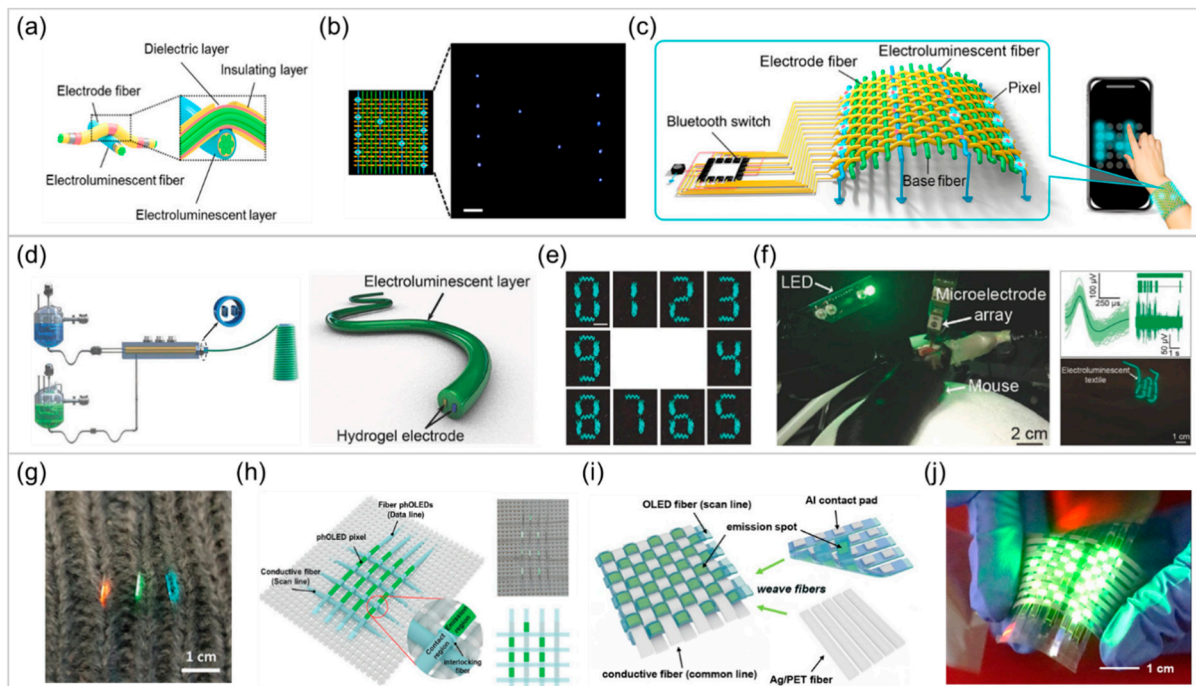


Figure 6. (a) Schematic illustration of a pixel structure in the electroluminescent fabric. (b) Schematic illustration and photograph of the electroluminescent fabric showing the pattern “N”. (c) Schematic illustration of the smart electroluminescent fabric being functionalized by connecting Bluetooth. (a–c) Reproduced with permission Ref. [65]. Copyright 2021, American Chemical Society. (d) Schematics of the simultaneous extrusion process and the light-emitting fiber (e) Photograph of an electroluminescent textile displaying numbers from 0 to 9. (f) Photograph of the real-time brain-interfaced camouflage of the fiber under green illumination. (d–f) Reproduced with permission Ref. [66]. Copyright 2018, Wiley-VCH. (g) Photograph of the RGB fiber PELDs, which are woven into clothes. (h) Left: schematic illustration of the textile display and a magnified schematic showing the contact region, the emission region, and the interlocking fiber. Right: photograph of the resulting textile display, which is integrated into the textile, visualizing the letter information “A”. (g,h) Reproduced with permission Ref. [15]. Copyright 2021, Wiley-VCH. (i) Schematic illustration of the woven OLED textile display consisting of orthogonally arranged arrays of interconnectable OLED fibers and conductive fibers. (j) Photograph of the working woven textile device comprising 10×10 fiber arrays by the passive matrix scheme. (i,j) Reproduced with permission Ref. [67]. Copyright 2021, American Chemical Society.

Hwang et al. fabricated 1D cylinder-shaped red, green, and blue PELDs on a polyethylene terephthalate (PET) fiber substrate, using a multiple-dip coating method (Figure 6g) [15]. The PELD fibers exhibited excellent optoelectronic performance, including good brightness (4462 , $11,482$, and 1199 cd m^{-2} for red, green, and blue, respectively), high current efficiency, and low driving voltages of $< 8 \text{ V}$, compared with those of conventional OLEDs on glass substrates [15]. Specifically, they showed the highest values of current efficiency at 16.3 , 60.7 , and 16.9 cd A^{-1} for red, green, and blue, respectively [15]. In addition, the proposed PELDs operated after repetitive flexural tests in multiple directions, as well as under 1.75% tensile strain [15]. The PELD fibers were used as independent pixels in an addressable structure and could be operated using a passive matrix scheme [15]. Letter information was successfully visualized on garments woven of the PELD fibers, indicating their potential to realize wearable textile displays (Figure 6h) [15].

Despite this progress, developing wearable displays composed of luminescent textiles still needs to be performed to achieve high electroluminescence performance, robust interconnection of lighting fibers, and a durable passivation layer. To address the aforementioned issues, Song et al. reported a feasible strategy for OLED textile displays that

comprise interconnectable phosphorescent OLED fibers and a polyurethane (PU)-based passivation layer (Figure 6i) [64]. The green OLEDs, in a 1D OLED pixel array, were thermally deposited onto the ITO/PET rectangular fibers with a patterned PU side barrier [67]. They exhibited a high brightness of $\sim 4300 \text{ cd m}^{-2}$ at 5 V, and an efficiency of $\sim 46 \text{ cd A}^{-1}$ ($\sim 58 \text{ lm W}^{-1}$), with environmental robustness [67]. The woven OLED network and perpendicularly aligned conductive fibers were driven by a passive matrix driving process, and, moreover, operated even under the water and under stretch deformation along the diagonal axis (Figure 6j) [67]. However, further research on light-emitting fibers needs to progress to realize low diameter, 360° light emissions, and a simple manufacturing process developed for practical wearable displays.

3.4. Energy-Harvesting/Storage Devices

Stiff and rigid batteries and energy harvesting devices hinder the development of wearable devices, which require flexibility [68]. Batteries with high capacity, a long-term cycling life, and energy-generating capabilities are also needed to build higher-level wearable electronic systems that include logic circuits [68]. Large-scale quantitative data transfer and computing consume a great deal of power. Therefore, it is important to develop deformable and durable energy harvesting/storage devices with high energy density. To meet the requirements of wearables, fibriform energy harvesting and storage devices have been demonstrated during the past decade. In this section, we describe recent efforts to develop fiber-shaped energy harvesting and storage devices.

Given that portable batteries have gradually become important in the wearable device industry, fiber-shaped batteries should have high capacities, long lifetimes, and excellent mechanical robustness. Recently, various shapes and materials have been used to realize fiber batteries. Both fiber-shaped lithium- and sodium-ion batteries with 3D interconnected hexagonal structures have been developed, using exclusive ion transport and efficient pseudocapacitive charge storage [69]. Li et al. developed a washable zinc-ion battery (ZIB) using double-helix yarn electrodes and a polyacrylamide electrolyte [70]. The yarn ZIB exhibits a high specific capacity (302 mAh g^{-1}) and volumetric energy density (54 mWh cm^{-3}), as well as excellent knittability and stretchability (up to 300% strain) [70]. Owing to its tailorable properties, long-yarn ZIB was woven into a textile that was used to power a flexible LED belt [70]. High-capacity aqueous zinc-ion battery fibers were also reported by Liao et al. (Figure 7a) [69]. The fibrous Zn-ion batteries, composed of V_6O_{13} /CNTs, can harvest energy from ambient air to recharge without an additional power supply (Figure 7b) [69]. The resulting battery fibers presented a high specific capacity (371 mAh g^{-1} at 200 mA g^{-1}), stable switching (>5000 cycles at 5 A g^{-1}) and recharging of $\sim 60\%$ upon exposure to air (Figure 7c) [69]. The self-charging battery fiber also acted as a strain sensor in an integrated wearable fingertip device (Figure 7d) [69].

For sustainable and self-sufficient use, energy harvesting technologies that can generate electric energy from the human body and its surroundings are required [71,72]. TENGs convert mechanical energy into electricity by triboelectrification and electrostatic induction. Wearable TENGs can collect low-frequency and irregular mechanical energy from body motion [73]. In previous research, fiber TENGs used thread-like metal wires, but those TENGs exhibited mechanical limitations such as low stretchability and elasticity. Although designing 2D or 3D textile architectures by knitting, weaving, or braiding different fiber TENGs can improve their deformability, the individual fibers remain mostly undeformed [73]. Lai et al. fabricated intrinsically stretchable fiber TENGs ($>650\%$ strain) that can harvest mechanical and electromagnetic energy (Figure 7e–g) [73]. Poly(styrene-*b*-(ethylene-co-butylene)-*b*-styrene) hollow elastomeric fibers filled with liquid metal EGaIn produced energy through triboelectricity (160 V m^{-1} and $\sim 360 \mu\text{W m}^{-1}$) and induced the electrification of the liquid metal ($\pm 8 \text{ V m}^{-1}$ at 60 Hz and $\sim 8 \mu\text{W m}^{-1}$) [73]. The fibers acted as textile power supplies and sensors self-powered by touch and motion (Figure 7h) [73].

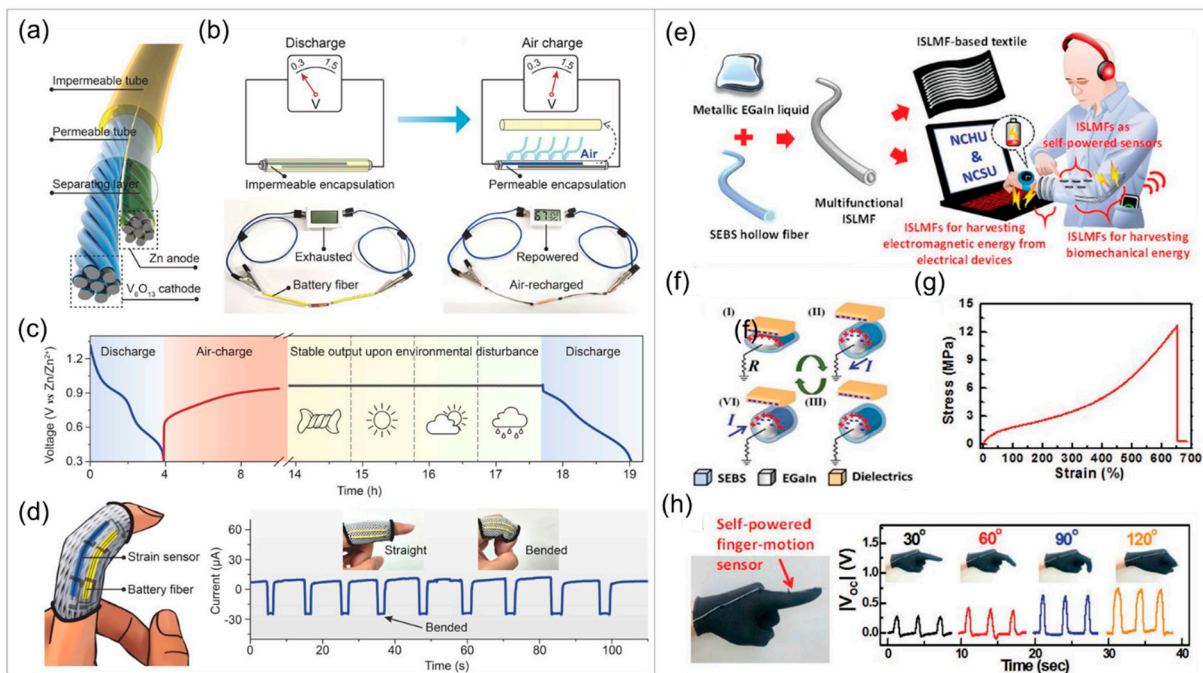


Figure 7. (a) Schematic of the double-layer-encapsulated Zn-ion battery fiber. (b) A thermometer powered by two air-rechargeable VCF/Zn battery fibers connected in series, shown in exhausted (left) and air-recharged (right) states, respectively. (c) The air-rechargeable VCF/Zn battery fiber presents stable voltage output under various environmental disturbances. (d) Left: schematic illustration of a strain sensor fiber powered by VCF/Zn battery fibers integrated in a flexible fingertip. Right: current-time curve of the strain sensor fiber upon the increasing bending cycle. (a–d) Reproduced with permission Ref. [69]. Copyright 2021, Royal Society of Chemistry. (e) Schematics of the fabrication process of the fiber TENG and its uses in collecting ambient energy and self-powered sensing. (f) Schematic illustration of the working mechanism for collecting energy from human motion. (g) Stress–strain curve of the fiber TENG. (h) Left: photograph of the fiber TENG as a self-powered finger-motion sensor. Right: real-time outputs when a finger is bent at different angles. (e–h) Reproduced with permission Ref. [73]. Copyright 2021, Wiley-VCH.

To integrate various functions in a single fiber and realize versatile energy fibers, Han et al. fabricated a multifunctional coaxial energy fiber for energy generation, storage, and use [74]. The energy fiber comprises a fiber-shaped TENG, supercapacitor, and pressure sensor in a coaxial geometry [74]. Each energy unit showed a length-specific capacitance density of 13.42 mF cm^{-1} , stable charging/discharging cycling ($\sim 96.6\%$ loss), maximum power generation of $2.5 \text{ }\mu\text{W}$, and good tactile sensitivity of 1.003 V kPa^{-1} (below 23 kPa) [74]. The demonstration of a soft and multifunctional energy fiber makes it an attractive option for human–machine interactive systems, intelligent robots, and smart tactile-sensing clothes [74].

Among promising energy storage devices for future wearable applications, fiber-shaped supercapacitors have attracted significant attention in recent years due to their good electrochemical stability under mechanical deformation. They can be easily assembled into 3D fabric structures and integrate into cloth by traditional textile forming processes [75]. Yu et al. fabricated textile-based supercapacitors (TSCs) on different types of textile fabrics using additive functionalization and embroidery manufacturing (AFEM) [75]. High areal energy storage and power capabilities of TSCs were demonstrated with various electrode materials, device structures, pattern designs, and array connections during the AFEM process [75]. The AFEM-fabricated TSCs show high potential for mass production in the near future [75].

Cloths protect human skin from the external environment and absorb solar energy. Fiber-shaped and fabric-based solar cells, another important energy-harvesting device for wearables, have recently been demonstrated: organic solar cells [76], dye-sensitized solar cells [77,78], and perovskite photovoltaics [79,80] based on coaxial and twisted fiber struc-

tures. Many efforts have been made to demonstrate fiber solar cells that are lightweight, soft, flexible, portable, and mechanically robust. Fiber-shaped solar cells in woven structures could improve overall power output.

We expect future garments to be made from energy-harvesting and storage textiles that will be used as primary power sources for wearable devices in daily life, although that could require a technical revolution.

4. Integrated Smart Electronic Textiles

Integrated wearable systems offer promising opportunities to continuously monitor a user's surrounding environment and health. Furthermore, they facilitate communication, external-environment sensing, and power generation and supply. Recent research has focused on combinations of processors, sensors, displays, and energy systems to provide more reliable and accurate information [46].

The fiber-shaped device structure provides attractive possibilities in electronics. For example, electronic fibers could be integrated into a single device that could convert human/environmental information into electrical signals and then process those data. When the electrical fiber components are woven together into e-textiles, they are connected in parallel or series to improve the output current and scale-down. Although 1D electronic devices output a limited current, an integrated system could maximize the electrical performance. The multi-functionalization and integration of 1D devices are required if e-textiles are to have broad applications. For instance, an integrated fiber-shaped supercapacitor and sensor could monitor the wearer's health and external environment without requiring an external power source. Accordingly, self-powered electronic devices have also attracted considerable attention due to their potential for application in wearable monitoring technology and personalized intelligent systems [81,82]. Two fiber-shaped devices could be twisted to produce a 1D electronic system and then integrated by connecting a common electrode to form a 2D configuration that can function as both an energy harvester and an electronic device. Such a design strategy represents one promising avenue for future electronics. Although other considerations, such as comfort and washability, are important for wearable electronics, the performance and function of integrated e-textiles is already advancing.

As a bridge to interaction in human-portable devices, display textiles offer a real-time communication function that could help reduce a user's difficulties in speech or speaking [66]. Recently, Shi et al. wove a large-area display textile based on electroluminescent units formed at the weft-warp contact points within the fabric (Figure 8a) [20]. The solution-processed luminescent warp and conductive weft fibers contained ZnS phosphor dispersed in an insulating polymer, and ionic-liquid-doped polyurethane gel, respectively [20]. A multifunctional integrated textile system was then demonstrated by weaving that display textile with a fiber-based keyboard and power supply (Figure 8b) [20]. This integrated e-textile showed useful communication and interactive navigation display functions (Figure 8c) [20]. Such smart textiles could be used as wearable communication tools in the future.

Wearable sensory interfaces that can record, model, and understand human-environment interactions are important in the development of wearable healthcare and robotics. Luo et al. combined fiber-shaped sensors with machine learning to process and interpret a mass of tactile data [83]. The piezoresistive fibers comprised 3-ply stainless-steel threads coated with graphite nanoparticles, copper nanoparticles, and polydimethylsiloxane elastomer [83]. The functional fibers in a core-sheath structure could be woven into large-scale textiles using digital machine knitting (Figure 8d) [83]. To learn diverse human-environment interactions through tactile textiles, computational workflows based on AI have also been developed [83]. The AI-powered smart textiles can classify the sitting poses and motions of their human users (Figure 8e) [83]. The demonstration of tactile learning using a textile platform is expected to be applicable to cognitive science and the imitation learning of intelligent robots [83].

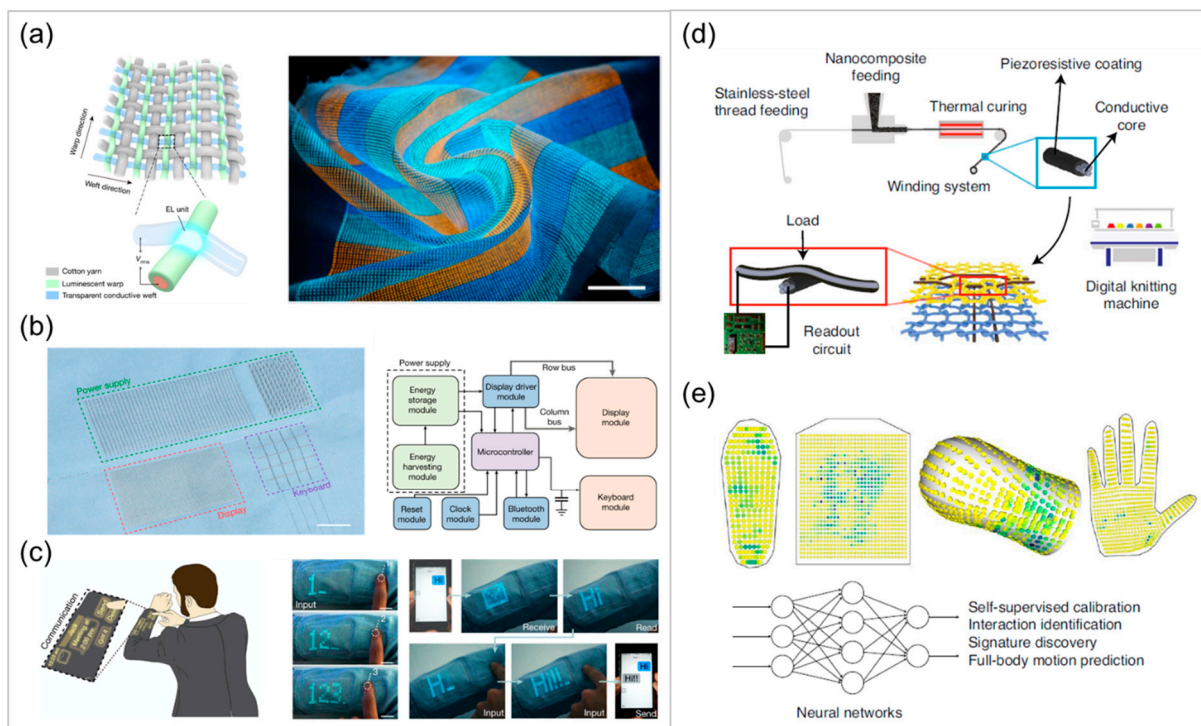


Figure 8. (a) Left: Schematic of the woven display textile. Each contacting luminescent warp and transparent conductive weft forms an EL unit (inset). Right: photograph of a multicolor display textile under complex deformations. (b) Left: photograph of an integrated textile system composed of display, information input, and power supply modules. Right: system-level block diagram of the integrated textile system (c) Left: conceptual illustration presents the idea that textiles integrated with a display and keyboard can be used as a communication platform. Middle: information is input onto the clothing by pressing the keys that are woven into the textile. Right: receiving and sending messages between the integrated textile system and a smartphone. (a–c) Reproduced with permission Ref. [20]. Copyright 2021, Springer Nature. (d) Schematic illustration of the scalable manufacturing of tactile sensing textiles using a customized coaxial piezoresistive fiber fabrication system and digital machine knitting. A commercial conductive stainless-steel thread is coated with a piezoresistive nanocomposite. (e) Examples of tactile frames collected during human–environment interactions, and their applications explored using machine learning techniques. (d,e) Reproduced with permission Ref. [83]. Copyright 2021, Springer Nature.

Using existing technology, e-textiles have been fabricated through complex and delicate multistep processes, the costs of which are very high. The way to address that issue is to find suitable e-textile weaving techniques and reduce the number of production steps to reduce costs. For instance, instead of adding functionality to an existing fabric, building functional fibers into a fabric would make the e-textiles more comfortable to wear and simplify their production. However, to realize large-scale applications, e-textile techniques based on commercial weaving machines should be developed, and the durability of the electronic fibers must be robust.

5. Challenges and Outlook

During the past decade, research into 1D electronic devices has grown rapidly due to their potential as promising structural and functional components of future electronics. However, fiber electronics still suffer from several problems, such as high power consumption, low integration density, poor mechanical and environmental stability, and complex fabrication methods [35]. For instance, FETs using fiber and textile structures show low field-effect mobilities and low on-current states that offer considerably worse performance than those made using flexible planar substrates. Therefore, the electrical performance of 1D devices needs to be improved, while maintaining fiber structures with good mechanical properties. Additionally, 1D devices should be protected by encapsulation because of the

high sensitivity of many active and electrode materials to oxygen and moisture in the atmosphere, which could accelerate device degradation [2].

Another critical issue in the field of fiber electronics is developing suitable electrodes and a predominant technology for connecting 1D devices. Most emerging wearable devices include many connecting electrodes that interact with other functional devices. Those interactions exchange information between the external environment and the human body. Electrode materials are typically more rigid than either human bodies or fabric. Therefore, wearable electrodes must be made to withstand human motion, moisture, and the mechanical stress of deforming fabric. Designing and interfacing electrodes with soft materials are thus one of the major barriers to the implementation of electronic fibers.

Wearable electrodes surrounded by active layers need to be structurally stable to prevent disconnection, delamination, and cracks during deformation. Although 1D stretchable and flexible electrodes have been studied extensively, their long-term stability is much lower than expected. Despite the realization of various stretchable systems, effective long-term connections between circuit elements in fiber systems are still technically difficult. On the one hand, it is extremely important to find new and efficient conductive threads that can be industrially woven or knit. On the other hand, comfortable and stable electrodes that are suitable for fiber substrates should be developed to realize their practical applications. Reliable operation and long-term durability, such as resistance to washing and temperature changes, are also important requirements to meet before smart e-textiles can be blended into garments. To meet those demands, diverse strategies, such as nanostructured surfaces and chemical treatments, should be used to modify the active layers and improve electrical performance.

Optimizing the e-textile configuration and its electrode connection is important to maximize their electrical performance. The interface between active materials and electrodes in a textile structure, as well as that between neighboring fibers and electrodes, influences the charge transfer properties of 1D electronic fibers. Even though all electronic devices depend on charge injection and transport, when weaving warps and wefts, it is difficult to provide sufficiently good ohmic contact, due to the rough and loose structure of textiles that can deform in varied and unpredictable ways [20].

In conclusion, electronic fibers and their corresponding smart integrated electronic systems have been shown to be feasible for wearable electronics. The development of fiber materials, fabrication methods, textile integration, and structural engineering should proceed to enable the implementation of wearable electronic systems invisible to users. Future wearables could evaluate changes in health and external environments. Such wearable, integrated electronic systems would then become a new category of clothing products.

Author Contributions: Conceptualization, writing—M.K., T.-W.K. Both authors have read and agreed to the published version of the manuscript.

Funding: This study was supported by the National Research Foundation of Korea (2020R1A2C2010163).

Institutional Review Board Statement: Not applicable.

Informed Consent Statement: Not applicable.

Data Availability Statement: The data presented in this study are openly available in reference number [3,15,20,22,26,29,30,34,35,41,45,47,61,65–67,69,73,83].

Conflicts of Interest: The authors declare no conflict of interest.

References

1. Lee, J.; Jeon, S.; Seo, H.; Lee, J.T.; Park, S. Fiber-Based Sensors and Energy Systems for Wearable Electronics. *Appl. Sci.* **2021**, *11*, 531. [[CrossRef](#)]
2. Heo, J.S.; Eom, J.; Kim, Y.H.; Park, S.K. Recent progress of textile-based wearable electronics: A comprehensive review of materials, devices, and applications. *Small* **2018**, *14*, 1703034. [[CrossRef](#)]

3. Kang, M.; Lee, S.-A.; Jang, S.; Hwang, S.; Lee, S.-K.; Bae, S.; Hong, J.-M.; Lee, S.H.; Jeong, K.-U.; Lim, J.A. Low-voltage organic transistor memory fiber with a nanograined organic ferroelectric film. *ACS Appl. Mater. Interfaces* **2019**, *11*, 22575–22582. [[CrossRef](#)] [[PubMed](#)]
4. Zeng, W.; Shu, L.; Li, Q.; Chen, S.; Wang, F.; Tao, X.M. Fiber-based wearable electronics: A review of materials, fabrication, devices, and applications. *Adv. Mater.* **2014**, *26*, 5310–5336. [[CrossRef](#)]
5. Shi, Q.; Sun, J.; Hou, C.; Li, Y.; Zhang, Q.; Wang, H. Advanced functional fiber and smart textile. *Adv. Fiber Mater.* **2019**, *1*, 3–31. [[CrossRef](#)]
6. Yan, W.; Page, A.; Nguyen-Dang, T.; Qu, Y.; Sordo, F.; Wei, L.; Sorin, F. Advanced multimaterial electronic and optoelectronic fibers and textiles. *Adv. Mater.* **2019**, *31*, 1802348. [[CrossRef](#)]
7. Trung, T.Q.; Le, H.S.; Dang, T.M.L.; Ju, S.; Park, S.Y.; Lee, N.E. Freestanding, Fiber-Based, Wearable Temperature Sensor with Tunable Thermal Index for Healthcare Monitoring. *Adv. Healthc. Mater.* **2018**, *7*, 1800074. [[CrossRef](#)] [[PubMed](#)]
8. Zhu, M.; Lou, M.; Abdalla, I.; Yu, J.; Li, Z.; Ding, B. Highly shape adaptive fiber based electronic skin for sensitive joint motion monitoring and tactile sensing. *Nano Energy* **2020**, *69*, 104429. [[CrossRef](#)]
9. Souri, H.; Bhattacharyya, D. Highly stretchable multifunctional wearable devices based on conductive cotton and wool fabrics. *ACS Appl. Mater. Interfaces* **2018**, *10*, 20845–20853. [[CrossRef](#)]
10. Zhang, Y.; Bai, W.; Ren, J.; Weng, W.; Lin, H.; Zhang, Z.; Peng, H. Super-stretchy lithium-ion battery based on carbon nanotube fiber. *J. Mater. Chem. A* **2014**, *2*, 11054–11059. [[CrossRef](#)]
11. Lin, H.; Weng, W.; Ren, J.; Qiu, L.; Zhang, Z.; Chen, P.; Chen, X.; Deng, J.; Wang, Y.; Peng, H. Twisted aligned carbon nanotube/silicon composite fiber anode for flexible wire-shaped lithium-ion battery. *Adv. Mater.* **2014**, *26*, 1217–1222. [[CrossRef](#)]
12. Zhang, Q.; Sun, J.; Pan, Z.; Zhang, J.; Zhao, J.; Wang, X.; Zhang, C.; Yao, Y.; Lu, W.; Li, Q. Stretchable fiber-shaped asymmetric supercapacitors with ultrahigh energy density. *Nano Energy* **2017**, *39*, 219–228. [[CrossRef](#)]
13. Rein, M.; Favrod, V.D.; Hou, C.; Khudiyev, T.; Stolyarov, A.; Cox, J.; Chung, C.-C.; Chhav, C.; Ellis, M.; Joannopoulos, J. Diode fibres for fabric-based optical communications. *Nature* **2018**, *560*, 214–218. [[CrossRef](#)] [[PubMed](#)]
14. Chen, M.; Wang, Z.; Li, K.; Wang, X.; Wei, L. Elastic and stretchable functional fibers: A review of materials, fabrication methods, and applications. *Adv. Fiber Mater.* **2021**, 1–13. [[CrossRef](#)]
15. Hwang, Y.H.; Kwon, S.; Shin, J.B.; Kim, H.; Son, Y.H.; Lee, H.S.; Noh, B.; Nam, M.; Choi, K.C. Bright-Multicolor, Highly Efficient, and Addressable Phosphorescent Organic Light-Emitting Fibers: Toward Wearable Textile Information Displays. *Adv. Funct. Mater.* **2021**, *31*, 2009336. [[CrossRef](#)]
16. Sun, H.; Zhang, Y.; Zhang, J.; Sun, X.; Peng, H. Energy harvesting and storage in 1D devices. *Nat. Rev. Mater.* **2017**, *2*, 1–12. [[CrossRef](#)]
17. Zhou, Y.; Fang, J.; Zhao, Y.; Lin, T. Fiber-Shaped Electronic Devices. *Handb. Fibrous Mater.* **2020**, 557–591. [[CrossRef](#)]
18. Loke, G.; Yan, W.; Khudiyev, T.; Noel, G.; Fink, Y. Recent progress and perspectives of thermally drawn multimaterial fiber electronics. *Adv. Mater.* **2020**, *32*, 1904911. [[CrossRef](#)]
19. Yan, W.; Dong, C.; Xiang, Y.; Jiang, S.; Leber, A.; Loke, G.; Xu, W.; Hou, C.; Zhou, S.; Chen, M. Thermally drawn advanced functional fibers: New frontier of flexible electronics. *Mater. Today* **2020**. [[CrossRef](#)]
20. Shi, X.; Zuo, Y.; Zhai, P.; Shen, J.; Yang, Y.; Gao, Z.; Liao, M.; Wu, J.; Wang, J.; Xu, X. Large-area display textiles integrated with functional systems. *Nature* **2021**, *591*, 240–245. [[CrossRef](#)]
21. Kim, H.M.; Kang, H.W.; Hwang, D.K.; Lim, H.S.; Ju, B.K.; Lim, J.A. Metal–Insulator–Semiconductor Coaxial Microfibers Based on Self-Organization of Organic Semiconductor: Polymer Blend for Weavable, Fibriform Organic Field-Effect Transistors. *Adv. Funct. Mater.* **2016**, *26*, 2706–2714. [[CrossRef](#)]
22. Heo, J.S.; Kim, T.; Ban, S.G.; Kim, D.; Lee, J.H.; Jur, J.S.; Kim, M.G.; Kim, Y.H.; Hong, Y.; Park, S.K. Thread-Like CMOS Logic Circuits Enabled by Reel-Processed Single-Walled Carbon Nanotube Transistors via Selective Doping. *Adv. Mater.* **2017**, *29*, 1701822. [[CrossRef](#)]
23. Yoon, S.S.; Lee, K.E.; Cha, H.-J.; Seong, D.G.; Um, M.-K.; Byun, J.-H.; Oh, Y.; Oh, J.H.; Lee, W.; Lee, J.U. Highly conductive graphene/Ag hybrid fibers for flexible fiber-type transistors. *Sci. Rep.* **2015**, *5*, 1–12. [[CrossRef](#)]
24. Hamedi, M.; Herlogsson, L.; Crispin, X.; Marcilla, R.; Berggren, M.; Inganäs, O. Fiber-embedded electrolyte-gated field-effect transistors for e-textiles. *Adv. Mater.* **2009**, *21*, 573–577. [[CrossRef](#)]
25. Zheng, L.; Wang, C.; Tian, X.; Zhang, X.; Dong, H.; Hu, W. A general route towards two-dimensional organic crystal-based functional fibriform transistors for wearable electronic textiles. *J. Mater. Chem. C* **2021**, *9*, 472–480. [[CrossRef](#)]
26. Owyung, R.E.; Terse-Thakoor, T.; Rezaei Nejad, H.; Panzer, M.J.; Sonkusale, S.R. Highly flexible transistor threads for all-thread based integrated circuits and multiplexed diagnostics. *ACS Appl. Mater. Interfaces* **2019**, *11*, 31096–31104. [[CrossRef](#)]
27. Park, J.W.; Kwon, S.; Kwon, J.H.; Kim, C.Y.; Choi, K.C. Low-Leakage Fiber-Based Field-Effect Transistors with an Al₂O₃–MgO Nanolaminate as Gate Insulator. *ACS Appl. Electron. Mater.* **2019**, *1*, 1400–1407. [[CrossRef](#)]
28. Park, C.J.; Heo, J.S.; Kim, K.-I.; Yi, G.; Kang, J.; Park, J.S.; Kim, Y.-H.; Park, S.K. 1-Dimensional fiber-based field-effect transistors made by low-temperature photochemically activated sol-gel metal-oxide materials for electronic textiles. *RSC Adv.* **2016**, *6*, 18596–18600. [[CrossRef](#)]
29. Kim, H.; Kang, T.-H.; Ahn, J.; Han, H.; Park, S.; Kim, S.J.; Park, M.-C.; Paik, S.-h.; Hwang, D.K.; Yi, H. Spirally Wrapped Carbon Nanotube Microelectrodes for Fiber Optoelectronic Devices beyond Geometrical Limitations toward Smart Wearable E-Textile Applications. *ACS Nano* **2020**. [[CrossRef](#)]

30. Kim, S.J.; Kim, H.; Ahn, J.; Hwang, D.K.; Ju, H.; Park, M.C.; Yang, H.; Kim, S.H.; Jang, H.W.; Lim, J.A. A new architecture for fibrous organic transistors based on a double-stranded assembly of electrode microfibers for electronic textile applications. *Adv. Mater.* **2019**, *31*, 1900564. [[CrossRef](#)]
31. Zhang, L.; Andrew, T. Vapor-Coated Monofilament Fibers for Embroidered Electrochemical Transistor Arrays on Fabrics. *Adv. Electron. Mater.* **2018**, *4*, 1800271. [[CrossRef](#)]
32. Rivnay, J.; Inal, S.; Salleo, A.; Owens, R.M.; Berggren, M.; Malliaras, G.G. Organic electrochemical transistors. *Nat. Rev. Mater.* **2018**, *3*, 1–14. [[CrossRef](#)]
33. Kang, T.-K. Highly stretchable non-volatile nylon thread memory. *Sci. Rep.* **2016**, *6*, 1–7. [[CrossRef](#)] [[PubMed](#)]
34. Jo, A.; Seo, Y.; Ko, M.; Kim, C.; Kim, H.; Nam, S.; Choi, H.; Hwang, C.S.; Lee, M.J. Textile resistance switching memory for fabric electronics. *Adv. Funct. Mater.* **2017**, *27*, 1605593. [[CrossRef](#)]
35. Bae, H.; Jang, B.C.; Park, H.; Jung, S.-H.; Lee, H.M.; Park, J.-Y.; Jeon, S.-B.; Son, G.; Tcho, I.-W.; Yu, K. Functional circuitry on commercial fabric via textile-compatible nanoscale film coating process for fibertronics. *Nano Lett.* **2017**, *17*, 6443–6452. [[CrossRef](#)]
36. Baeg, K.J.; Khim, D.; Kim, J.; Yang, B.D.; Kang, M.; Jung, S.W.; You, I.K.; Kim, D.Y.; Noh, Y.Y. High-performance top-gated organic field-effect transistor memory using electrets for monolithic printed flexible NAND flash memory. *Adv. Funct. Mater.* **2012**, *22*, 2915–2926. [[CrossRef](#)]
37. Chen, G.; Fang, Y.; Zhao, X.; Tat, T.; Chen, J. Textiles for learning tactile interactions. *Nat. Electron.* **2021**, *4*, 175–176. [[CrossRef](#)]
38. Bae, H.; Kim, D.; Seo, M.; Jin, I.K.; Jeon, S.B.; Lee, H.M.; Jung, S.H.; Jang, B.C.; Son, G.; Yu, K. Bioinspired Polydopamine-Based Resistive-Switching Memory on Cotton Fabric for Wearable Neuromorphic Device Applications. *Adv. Mater. Technol.* **2019**, *4*, 1900151. [[CrossRef](#)]
39. Moin, A.; Zhou, A.; Rahimi, A.; Menon, A.; Benatti, S.; Alexandrov, G.; Tamakloe, S.; Ting, J.; Yamamoto, N.; Khan, Y. A wearable biosensing system with in-sensor adaptive machine learning for hand gesture recognition. *Nat. Electron.* **2021**, *4*, 54–63. [[CrossRef](#)]
40. Zhou, F.; Chai, Y. Near-sensor and in-sensor computing. *Nat. Electron.* **2020**, *3*, 664–671. [[CrossRef](#)]
41. Xu, X.; Zhou, X.; Wang, T.; Shi, X.; Liu, Y.; Zuo, Y.; Xu, L.; Wang, M.; Hu, X.; Yang, X. Robust DNA-Bridged Memristor for Textile Chips. *Angew. Chem. Int. Ed.* **2020**, *59*, 12762–12768. [[CrossRef](#)]
42. Shao, L.; Zhao, Y.; Liu, Y. Organic Synaptic Transistors: The Evolutionary Path from Memory Cells to the Application of Artificial Neural Networks. *Adv. Funct. Mater.* **2021**. [[CrossRef](#)]
43. Park, Y.; Park, M.J.; Lee, J.S. Reduced Graphene Oxide-Based Artificial Synapse Yarns for Wearable Textile Device Applications. *Adv. Funct. Mater.* **2018**, *28*, 1804123. [[CrossRef](#)]
44. Choi, S.; Jang, S.; Moon, J.-H.; Kim, J.C.; Jeong, H.Y.; Jang, P.; Lee, K.-J.; Wang, G. A self-rectifying TaO_y/nanoporous TaO_x memristor synaptic array for learning and energy-efficient neuromorphic systems. *NPG Asia Mater.* **2018**, *10*, 1097–1106. [[CrossRef](#)]
45. Ham, S.; Kang, M.; Jang, S.; Jang, J.; Choi, S.; Kim, T.-W.; Wang, G. One-dimensional organic artificial multi-synapses enabling electronic textile neural network for wearable neuromorphic applications. *Sci. Adv.* **2020**, *6*, eaba1178. [[CrossRef](#)] [[PubMed](#)]
46. Lou, Z.; Wang, L.; Jiang, K.; Wei, Z.; Shen, G. Reviews of wearable healthcare systems: Materials, devices and system integration. *Mater. Sci. Eng. R Rep.* **2020**, *140*, 100523. [[CrossRef](#)]
47. Meng, K.; Zhao, S.; Zhou, Y.; Wu, Y.; Zhang, S.; He, Q.; Wang, X.; Zhou, Z.; Fan, W.; Tan, X. A wireless textile-based sensor system for self-powered personalized health care. *Matter* **2020**, *2*, 896–907. [[CrossRef](#)]
48. Ma, L.; Wu, R.; Liu, S.; Patil, A.; Gong, H.; Yi, J.; Sheng, F.; Zhang, Y.; Wang, J.; Wang, J. A Machine-Fabricated 3D Honeycomb-Structured Flame-Retardant Triboelectric Fabric for Fire Escape and Rescue. *Adv. Mater.* **2020**, *32*, 2003897. [[CrossRef](#)] [[PubMed](#)]
49. Wu, Y.; Yang, Y.; Li, C.; Li, Y.; Chen, W. Flexible and electroactive textile actuator enabled by PEDOT: PSS/MOF-derivative electrode ink. *Front. Bioeng. Biotechnol.* **2020**, *8*. [[CrossRef](#)] [[PubMed](#)]
50. Ding, T.; Chan, K.H.; Zhou, Y.; Wang, X.-Q.; Cheng, Y.; Li, T.; Ho, G.W. Scalable thermoelectric fibers for multifunctional textile-electronics. *Nat. Commun.* **2020**, *11*, 1–8. [[CrossRef](#)]
51. Liu, S.; Ma, K.; Yang, B.; Li, H.; Tao, X. Textile Electronics for VR/AR Applications. *Adv. Funct. Mater.* **2020**. [[CrossRef](#)]
52. Xu, X.; Xie, S.; Zhang, Y.; Peng, H. The rise of fiber electronics. *Angew. Chem. Int. Ed.* **2019**, *58*, 13643–13653. [[CrossRef](#)] [[PubMed](#)]
53. Wang, L.; Wang, L.; Zhang, Y.; Pan, J.; Li, S.; Sun, X.; Zhang, B.; Peng, H. Weaving sensing fibers into electrochemical fabric for real-time health monitoring. *Adv. Funct. Mater.* **2018**, *28*. [[CrossRef](#)]
54. Zhao, Y.; Zhai, Q.; Dong, D.; An, T.; Gong, S.; Shi, Q.; Cheng, W. Highly stretchable and strain-insensitive fiber-based wearable electrochemical biosensor to monitor glucose in the sweat. *Anal. Chem.* **2019**, *91*, 6569–6576. [[CrossRef](#)]
55. Li, W.; Chen, R.; Qi, W.; Cai, L.; Sun, Y.; Sun, M.; Li, C.; Yang, X.; Xiang, L.; Xie, D. Reduced graphene oxide/mesoporous ZnO NSs hybrid fibers for flexible, stretchable, twisted, and wearable NO₂ E-textile gas sensor. *ACS Sens.* **2019**, *4*, 2809–2818. [[CrossRef](#)]
56. Yun, Y.J.; Hong, W.G.; Choi, N.-J.; Kim, B.H.; Jun, Y.; Lee, H.-K. Ultrasensitive and highly selective graphene-based single yarn for use in wearable gas sensor. *Sci. Rep.* **2015**, *5*, 1–7.
57. Gumennik, A.; Stolyarov, A.M.; Schell, B.R.; Hou, C.; Lestoquoy, G.; Sorin, F.; McDaniel, W.; Rose, A.; Joannopoulos, J.D.; Fink, Y. All-in-fiber chemical sensing. *Adv. Mater.* **2012**, *24*, 6005–6009. [[CrossRef](#)]
58. Rui, K.; Wang, X.; Du, M.; Zhang, Y.; Wang, Q.; Ma, Z.; Zhang, Q.; Li, D.; Huang, X.; Sun, G. Dual-function metal–organic framework-based wearable fibers for gas probing and energy storage. *ACS Appl. Mater. Interfaces* **2018**, *10*, 2837–2842. [[CrossRef](#)]
59. Wang, R.; Zhai, Q.; Zhao, Y.; An, T.; Gong, S.; Guo, Z.; Shi, Q.; Yong, Z.; Cheng, W. Stretchable gold fiber-based wearable electrochemical sensor toward pH monitoring. *J. Mater. Chem. B* **2020**, *8*, 3655–3660. [[CrossRef](#)]

60. Madhu, S.; Anthuvan, A.J.; Ramasamy, S.; Manickam, P.; Bhansali, S.; Nagamony, P.; Chinnuswamy, V. ZnO nanorod integrated flexible carbon fibers for sweat cortisol detection. *ACS Appl. Electron. Mater.* **2020**, *2*, 499–509. [[CrossRef](#)]
61. Jia, Z.; Gong, J.; Zeng, Y.; Ran, J.; Liu, J.; Wang, K.; Xie, C.; Lu, X.; Wang, J. Bioinspired Conductive Silk Microfiber Integrated Bioelectronic for Diagnosis and Wound Healing in Diabetes. *Adv. Funct. Mater.* **2021**. [[CrossRef](#)]
62. Xu, X.; Chen, J.; Cai, S.; Long, Z.; Zhang, Y.; Su, L.; He, S.; Tang, C.; Liu, P.; Peng, H. A real-time wearable uv-radiation monitor based on a high-performance p-CuZnS/n-TiO₂ photodetector. *Adv. Mater.* **2018**, *30*. [[CrossRef](#)]
63. Kim, K.K.; Ha, I.; Won, P.; Seo, D.-G.; Cho, K.-J.; Ko, S.H. Transparent wearable three-dimensional touch by self-generated multiscale structure. *Nat. Commun.* **2019**, *10*, 1–8. [[CrossRef](#)]
64. Wang, L.; Fu, X.; He, J.; Shi, X.; Chen, T.; Chen, P.; Wang, B.; Peng, H. Application challenges in fiber and textile electronics. *Adv. Mater.* **2020**, *32*, 1901971. [[CrossRef](#)] [[PubMed](#)]
65. Mi, H.; Zhong, L.; Tang, X.; Xu, P.; Liu, X.; Luo, T.; Jiang, X. Electroluminescent Fabric Woven by Ultrastretchable Fibers for Arbitrarily Controllable Pattern Display. *ACS Appl. Mater. Interfaces* **2021**, *13*, 11260–11267. [[CrossRef](#)] [[PubMed](#)]
66. Zhang, Z.; Cui, L.; Shi, X.; Tian, X.; Wang, D.; Gu, C.; Chen, E.; Cheng, X.; Xu, Y.; Hu, Y. Textile display for electronic and brain-interfaced communications. *Adv. Mater.* **2018**, *30*. [[CrossRef](#)] [[PubMed](#)]
67. Song, Y.J.; Kim, J.-W.; Cho, H.-E.; Son, Y.H.; Lee, M.H.; Lee, J.; Choi, K.C.; Lee, S.-M. Fibertronic organic light-emitting diodes toward fully addressable, environmentally robust, wearable displays. *ACS Nano* **2020**, *14*, 1133–1140. [[CrossRef](#)]
68. Satharasinghe, A.; Hughes-Riley, T.; Dias, T. A Review of Solar Energy Harvesting Electronic Textiles. *Sensors* **2020**, *20*, 5938. [[CrossRef](#)] [[PubMed](#)]
69. Liao, M.; Wang, J.; Ye, L.; Sun, H.; Li, P.; Wang, C.; Tang, C.; Cheng, X.; Wang, B.; Peng, H. A high-capacity aqueous zinc-ion battery fiber with air-recharging capability. *J. Mater. Chem. A* **2021**, *9*, 6811–6818. [[CrossRef](#)]
70. Li, H.; Liu, Z.; Liang, G.; Huang, Y.; Huang, Y.; Zhu, M.; Pei, Z.; Xue, Q.; Tang, Z.; Wang, Y. Waterproof and tailorable elastic rechargeable yarn zinc ion batteries by a cross-linked polyacrylamide electrolyte. *ACS Nano* **2018**, *12*, 3140–3148. [[CrossRef](#)]
71. Mao, Y.; Li, Y.; Xie, J.; Liu, H.; Guo, C.; Hu, W. Triboelectric nanogenerator/supercapacitor in-one self-powered textile based on PTFE yarn wrapped PDMS/MnO₂NW hybrid elastomer. *Nano Energy* **2021**, *84*. [[CrossRef](#)]
72. Vasandani, P.; Gattu, B.; Wu, J.; Mao, Z.H.; Jia, W.; Sun, M. Triboelectric nanogenerator using microdome-patterned PDMS as a wearable respiratory energy harvester. *Adv. Mater. Technol.* **2017**, *2*. [[CrossRef](#)]
73. Lai, Y.C.; Lu, H.W.; Wu, H.M.; Zhang, D.; Yang, J.; Ma, J.; Shamsi, M.; Vallem, V.; Dickey, M.D. Elastic Multifunctional Liquid–Metal Fibers for Harvesting Mechanical and Electromagnetic Energy and as Self-Powered Sensors. *Adv. Energy Mater.* **2021**, *11*. [[CrossRef](#)]
74. Han, J.; Xu, C.; Zhang, J.; Xu, N.; Xiong, Y.; Cao, X.; Liang, Y.; Zheng, L.; Sun, J.; Zhai, J. Multifunctional Coaxial Energy Fiber toward Energy Harvesting, Storage, and Utilization. *ACS Nano* **2021**, *15*, 1597–1607. [[CrossRef](#)]
75. Huang, Q.; Wang, D.; Hu, H.; Shang, J.; Chang, J.; Xie, C.; Yang, Y.; Lepró, X.; Baughman, R.H.; Zheng, Z. Additive functionalization and embroidery for manufacturing wearable and washable textile supercapacitors. *Adv. Funct. Mater.* **2020**, *30*. [[CrossRef](#)]
76. Liu, D.; Li, Y.; Zhao, S.; Cao, A.; Zhang, C.; Liu, Z.; Bian, Z.; Liu, Z.; Huang, C. Single-layer graphene sheets as counter electrodes for fiber-shaped polymer solar cells. *RSC Adv.* **2013**, *3*, 13720–13727. [[CrossRef](#)]
77. Fan, X.; Chu, Z.; Wang, F.; Zhang, C.; Chen, L.; Tang, Y.; Zou, D. Wire-shaped flexible dye-sensitized solar cells. *Adv. Mater.* **2008**, *20*, 592–595. [[CrossRef](#)]
78. Hou, S.; Cai, X.; Fu, Y.; Lv, Z.; Wang, D.; Wu, H.; Zhang, C.; Chu, Z.; Zou, D. Transparent conductive oxide-less, flexible, and highly efficient dye-sensitized solar cells with commercialized carbon fiber as the counter electrode. *J. Mater. Chem.* **2011**, *21*, 13776–13779. [[CrossRef](#)]
79. Qiu, L.; Deng, J.; Lu, X.; Yang, Z.; Peng, H. Integrating perovskite solar cells into a flexible fiber. *Angew. Chem. Int. Ed.* **2014**, *53*, 10425–10428. [[CrossRef](#)]
80. He, S.; Qiu, L.; Fang, X.; Guan, G.; Chen, P.; Zhang, Z.; Peng, H. Radically grown obelisk-like ZnO arrays for perovskite solar cell fibers and fabrics through a mild solution process. *J. Mater. Chem. A* **2015**, *3*, 9406–9410. [[CrossRef](#)]
81. Zhu, M.; Yi, Z.; Yang, B.; Lee, C. Making use of nanoenergy from human–Nanogenerator and self-powered sensor enabled sustainable wireless IoT sensory systems. *Nano Today* **2021**, *36*. [[CrossRef](#)]
82. Chen, M.; Wang, Z.; Zhang, Q.; Wang, Z.; Liu, W.; Chen, M.; Wei, L. Self-powered multifunctional sensing based on super-elastic fibers by soluble-core thermal drawing. *Nat. Commun.* **2021**, *12*, 1–10.
83. Luo, Y.; Li, Y.; Sharma, P.; Shou, W.; Wu, K.; Foshey, M.; Li, B.; Palacios, T.; Torralba, A.; Matusik, W. Learning human–environment interactions using conformal tactile textiles. *Nat. Electron.* **2021**, *4*, 193–201. [[CrossRef](#)]